

Neutral-particle losses in the edge of spherical tokamaks

G P Maddison, G F Counsell, S J Fielding, P Helander,
H Meyer, K M Morel & D Reiter[†]

EURATOM/UKAEA Fusion Association,
Culham Science Centre, Abingdon, Oxon. OX14 3DB, UK.

[†] Heinrich-Heine-Universität Düsseldorf, Universitätstrasse 1, D-40225 Düsseldorf, Germany.

1. Introduction

A special feature of the spherical tokamaks START and its larger (~ 1 MA) successor MAST studied at Culham is their large ratio of vacuum tank to confined plasma volume, respectively ~ 20:1 and ~ 10:1. This space acts as a reservoir of neutral particles, supplied initially by the gas pre-fill, and replenished continuously by gas input and recycling. Consequently, interactions of neutral particles with the edge plasma can be abundant and exert a strong influence on behaviour. In addition to obvious effects on fuelling, it was also suggested by START data that they might help to disperse diverted power and so beneficially reduce target loads. A programme of modelling has therefore been inaugurated to examine such potential, and here preliminary findings are reported. The indicative observations from START are first outlined, before 2-D modelling of full-power MAST conditions is presented.

2. Illustration of START double-null plasma results

More recent START discharges, which eg achieved¹ record values of plasma β , were operated in an up-down symmetric double-null divertor configuration, with neutral-beam auxiliary heating. Power balance estimates, including radiation losses, for typical shots #35738 and #35745 ($I_p = 200$ kA, $B_0 = 0.3$ T, $R_0 = 30$ cm, $a = 23$ cm, $P_{NBI} = 0.87$ MW) disclose that ≈ 430 kW entered the scrape-off layers (SOLs) during their steadiest phases. On the other hand, measurements with Langmuir probes embedded in the four targets suggest, for equal

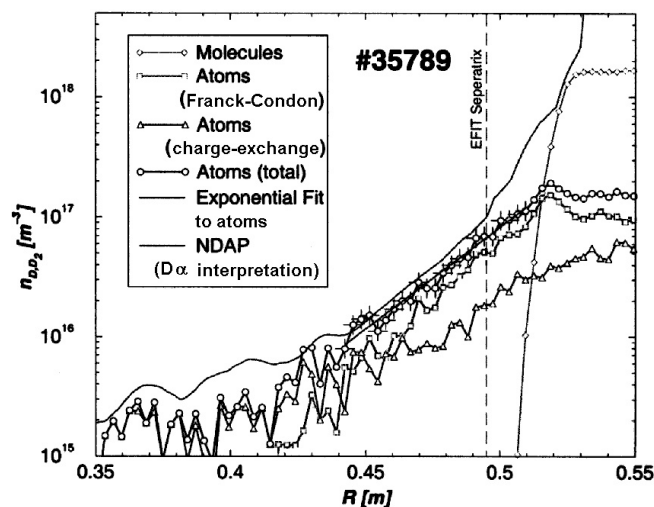


Fig.1 1-D Monte Carlo estimate of atom & molecule densities in the edge of START discharge #35789

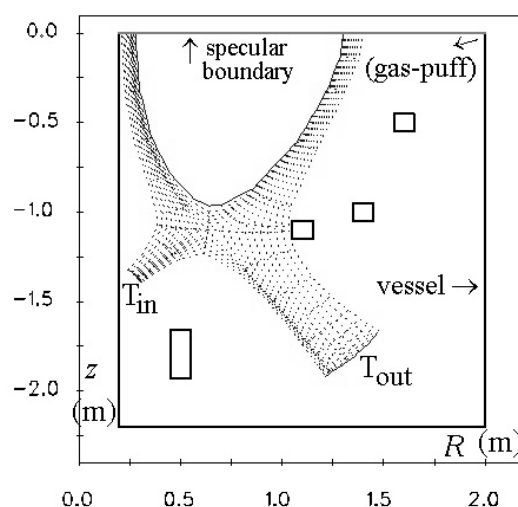


Fig.2 MAST lower-half DND geometry (including coil sections) used in "B2"+EIRENE calculations

temperature ions and electrons and ambipolar sheaths, the following deposited powers :-

	Inboard upper	Inboard lower	Outboard upper	Outboard lower
Power Q_t (kW)	12.4	14.1	62.3	48.0

Thus only $\approx 1/3$ of the efflux power appears at the targets; although differences in T_i^t and T_e^t and non-zero electric currents flowing in the edge could modify this figure, it is evident that some significant loss process intervenes along the SOLs. Furthermore, for anomalous transport of energy across the confined plasma which is driven just by flux-surface quantities and linearly by their spatial gradients, the expected outboard–inboard imbalance of double-null diverted powers is given by the purely geometric ratio of surface integrals² :-

$$Q^{\text{out}}/Q^{\text{in}} = (\int_{S_{\text{out}}} |\nabla\psi| dS) / (\int_{S_{\text{in}}} |\nabla\psi| dS) \quad . \quad (1)$$

In the START cases considered, this ratio is ≈ 14 , as opposed to that purely of toroidal areas $A_{\perp}^{\text{out}}/A_{\perp}^{\text{in}} = (\int_{S_{\text{out}}} dS) / (\int_{S_{\text{in}}} dS) \approx 3$. Note that this strong outboard prevalence due to Shafranov shift is a particular advantage of spherical tokamaks, as it helps to lessen loadings on their central column³. From (1), a total of ≈ 29 kW would therefore be expected at the START inboard targets above, close to the value measured, whereas ≈ 400 kW should reach the outboard side, of which only $\approx 1/4$ is ostensibly detected at the targets. Hence it is hinted that significant cooling occurs, principally within the outboard SOL where interactions with the surrounding envelope of neutral gas should be greatest.

In START, fast-ion gauge measurements usually showed gas densities of order $10^{18} \rightarrow 10^{19} \text{ m}^{-3}$ in its tank, eg substantially as a legacy of its pre-fill. Further support to this contributing to edge energy sinks is lent by 1-D Monte Carlo calculations with the code ‘NEUTRAL’, illustrated in Fig.1. These agree well with diagnostic interpretation of 1-D Balmer- α signals (labelled ‘NDAP’), and imply a considerable density of atoms within the SOL. More detailed 2-D modelling has therefore been undertaken to analyse associated losses for representative conditions in the new MAST device.

3. Modelling of MAST experiment

The MAST machine ($R = 0.7$ m, $a = 0.5$ m, $I_p \leq 2$ MA, $B_0 = 0.6$ T, $P_{\text{NBI}} \leq 5$ MW) will also operate primarily in double-null configuration, with NB heating. A sample discretization is plotted in Fig.2, prepared for the ‘B2’-EIRENE unified code suite⁴ assuming complete up-down and axi- symmetry. Note that in practice the divertor legs will extend completely to the central column and the top & bottom end-plates, but by-pass routes beneath the strike-points will still permit communication throughout the tank as in the test arrangement of Fig.2.

In addition to the pre-fill, over long MAST pulses (≤ 5 s) both gas-puffing and recycling will feed the gas density in its tank; the latter in particular will be favoured by the open divertor geometry first planned. To study its influence, coupled ‘B2’-EIRENE calculations have thus been performed assuming no neutral-particle sources other than 100% recycling at both targets, and no neutral-particle sinks other than re-entry back over the innermost magnetic surface included (ψ^{int}) into the core (where they are taken to be ionized), ie the vessel walls and coil cases are treated as fully saturated. Steady states are then achieved when these atomic escapes self-consistently balance the ion efflux derived, for boundary conditions of chosen innermost density n_e^{int} and the highest possible power efflux of $Q^{\text{int}} = 6$ MW split equally between electrons and ions. Three cases (A , B , C) have been solved, as defined in Table 1,

Lower half-system only (ie 3 MW total power)						
	Pure recycling, saturated walls			Recyc. + gas-puff & wall-pumping		
	Case A	Case B	Case C	Case A'	Case B'	Case C'
n_e^{int} (m^{-3})	2.e19	1.e20	2.e19	(test-particle runs on opposite background plasmas) ←		
$Q_e^{\text{int}}=Q_i^{\text{int}}$ (MW)	1.5	1.5	1.5			
$\chi^{e,i}/4=D_{\perp}$ ($\text{m}^2\cdot\text{s}^{-1}$)	0.2	0.2	4.0			
total flux amp. \mathcal{F}	6.	66.	10.			
Q_t^{out} (MW)	1.91	1.36	1.76			
Q_t^{in} (MW)	0.574	0.404	0.556			
$n_{\text{atom}}^{\text{tank}}$ (m^{-3})	3.53e16	3.44e17	1.15e17			
" $T_{\text{atom}}^{\text{tank}}$ " (eV)	12.7	7.78	10.9	12.8	7.88	11.2
$n_{\text{molecule}}^{\text{tank}}$ (m^{-3})	2.92e17	2.06e18	7.79e17	2.77e17	2.05e18	4.94e17
" $T_{\text{mol.}}^{\text{tank}}$ "(eV)	0.0374	0.0504	0.0452	0.0375	0.0520	0.0525
tot. P_e^{edge} loss (-) by neut. ints. (kW)	-42.1	-900.	-218.	-42.0	-914.	-199.
tot. P_i^{edge} loss (-) by neut. ints. (kW)	-466.	-335.	-219.	-471.	-395.	-198.
net mol. flux into (+) outboard (s^{-1})	9.43e20	1.01e21	3.98e21	1.30e21	1.44e22	2.39e21
net mol. flux into (+) inboard (s^{-1})	4.47e20	1.69e21	1.16e21	1.31e20	-7.74e19	2.30e20
net atom efflux from (-) outb. (s^{-1})	-2.07e21	-2.06e22	-9.08e21	-2.13e21	-2.16e22	-8.36e21
net atom en. flux from (-) outb.(kW)	-180.	-267.	-168.	-193.	-297.	-156.
net atom efflux from (-) inb. (s^{-1})	-7.10e20	-3.06e21	-1.21e21	-5.66e20	-2.50e21	-9.44e20
net atom en. flux from (-) inb.(kW)	-83.8	+2.41	-21.7	-70.7	+3.99	-18.2
tot. wall-pumping of atoms (s^{-1})	0	0	0	1.83e21	1.56e22	6.07e21

Table 1 Results of MAST "B2"-EIRENE and EIRENE "test-particle" calculations

scanning a range in edge density, and transport coefficients, from smaller JET-like quantities to larger Bohm-like ones. Recycling is measured by total flux amplification \mathcal{F} , ie total ion flux onto the targets divided by that crossing the innermost boundary ψ^{int} . This leads itself to appreciable neutral-particle density in the tank relative to the level for good transmission of the neutral beams ($\leq 1.5 \times 10^{18} \text{ m}^{-3}$). Electron and ion power losses shown are respective total sinks due to interactions with atoms, molecules and molecular ions in the whole calculation region. These are actually found to be small, except at high plasma density when recycling losses (radiation and ionization) dominate. Outboard to inboard target powers remain always close to the ratio of innermost surface areas, as imposed exactly at the coincident boundary condition ($Q^{\text{out}} / Q^{\text{in}} = 3.1$). Components of the losses carried by atom effluxes from the plasma are given separately for outboard and inboard sectors. A key point is the large fraction, often more than half, emerging through the private flux, so that specific divertor geometry must be important. Fluxes are of course larger through the larger outboard surface area.

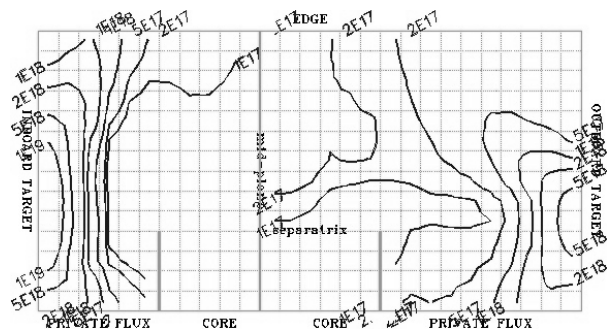


Fig.3 Molecule density (m^{-3}) shown over plasma computational map for Case A' (gas-puff+wall pump.)

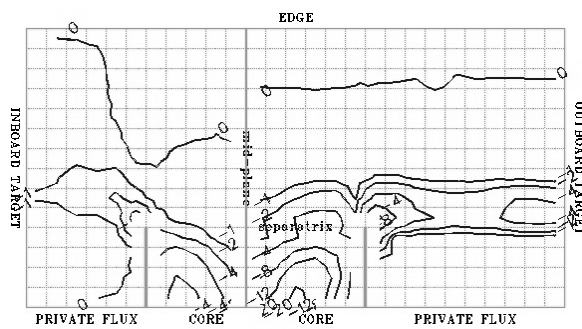


Fig.4 Ion energy sink per cell (kW) over plasma computational map for Case A' (gas-puff+wall pump.)

A more practical situation will involve a gas input to supplement fuelling, plus wall pumping of atoms, eg as after boronization. A first insight into such states has been inferred by adding a narrow gas-puff source of molecules at the vessel outboard mid-plane (see Fig.2) and no desorption of captured atoms at the vessel walls. Individual EIRENE calculations have then been executed using the former solutions as background plasmas: cases A' and C' injecting 10^{21} D_2 s^{-1} , case B' adding 10^{22} D_2 s^{-1} . Results are now not solved self-consistently, but are found in Table 1 to be generally quite close to the previous properties. Molecular fluxes are decreased at the inboard side, and increased outboard in cases A', B'; a drop in case C' is due to precedence of wall pumping. Observing that energy sinks and even atom effluxes are little altered implies that recycling dominates over puffing regarding neutral gas for these chosen MAST conditions. An illustration that molecules can penetrate into the SOL plasma is depicted for case A' in Fig.3. Particle and source/sink densities tend to be highest at the inboard strike-point, but to demonstrate where largest losses eg for ions actually occur, the accompanying sink due to neutral particles in each grid cell is plotted in Fig.4. Here it is strongest inside the separatrix within the confined region.

4. Summary

The vacuum tanks of the START and MAST spherical tokamaks provide large reservoirs of neutral particles which certainly affect plasma fuelling behaviour. Measurements in START also suggest strong cooling of the outboard SOL. Numerical 2-D modelling of representative MAST conditions, however, indicates that at least under strong auxiliary heating, energy losses from the diverted plasma would tend to be small; notably elastic-scattering and charge-exchange dispersal of power appear minor loss processes ($< 10\%$). Recycling sources of neutral particles dominate over likely levels of gas injection to assist fuelling, although high fractions of plasma effluxes occur through the private flux, and would therefore be susceptible to divertor geometry. Investigations will be extended to self-consistent calculations with gas-puffing and wall pumping, as well possibly as non-linear EIRENE applications to include self-collisions amongst the neutral particles.

This work was supported by the UK Department of Trade & Industry and Euratom.

References

1. M Gryaznevich *et al* Phys. Rev. Lett. 80 (1998) 3972
2. G P Maddison *et al* Proc. 18th EPS Conf. CFPP (Berlin, 1991) III-197
3. H R Wilson *et al* *this conference*
4. D Reiter J. Nuc. Mat. 196-198 (1992) 80